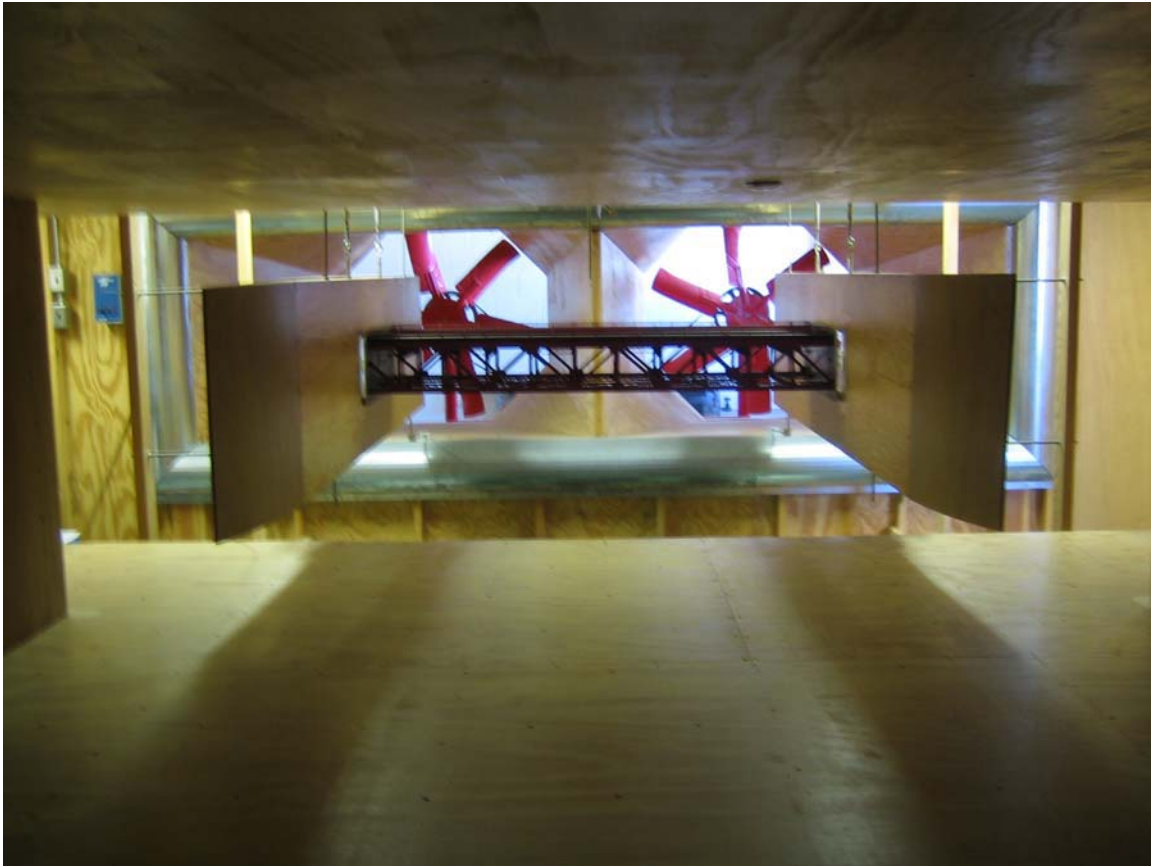


APPENDIX 5 MODELS

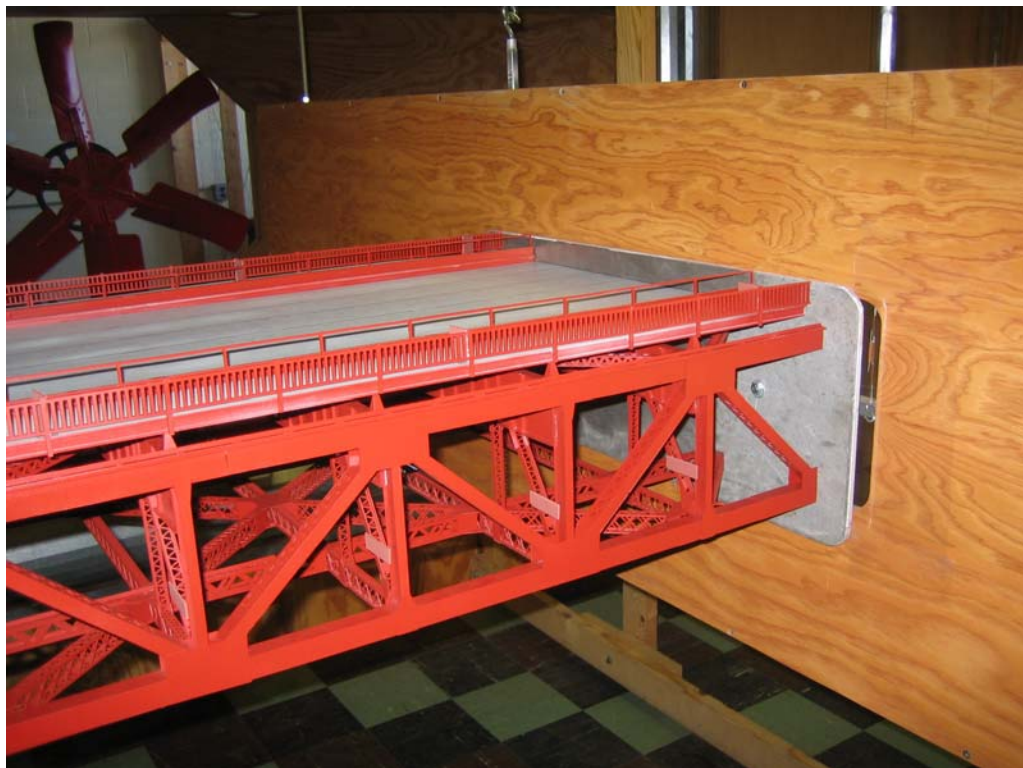
For this study the 1:50 scale model used in the previous study (Ref 2) was used. The model was lengthened to fit the new wind tunnel (see Appendix 2 - Facilities). The model is 1.6256 m long, which models a portion of the full-scale bridge deck 81.28 m (266.67 feet) long.

The model was made of laser cut plastic. As described in Appendices 3 and 4, the model needed to be geometrically correct only. Inertial and elastic scaling was not required.

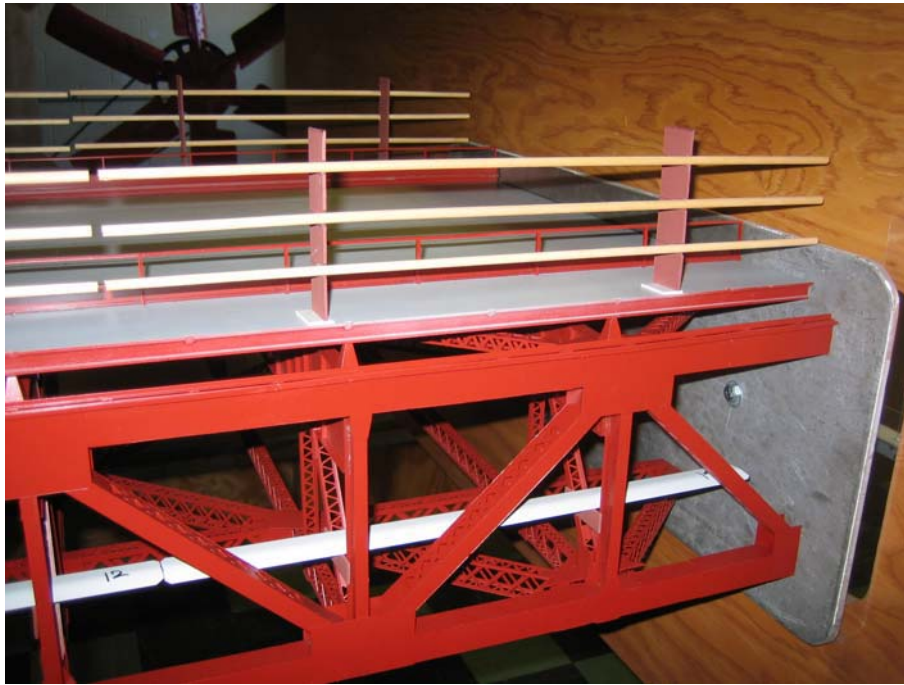
The model is shown in six configurations (the existing configuration and five suicide deterrent system configurations W0, W1, W1 (alternate), W2, W3, and W6) in the following photographs. Those configurations are defined in Section C.



Existing bridge (Test number W0)



Existing bridge (Test number W0)



Vertical 12' barrier with below deck winglets/catwalks (Test number W1)



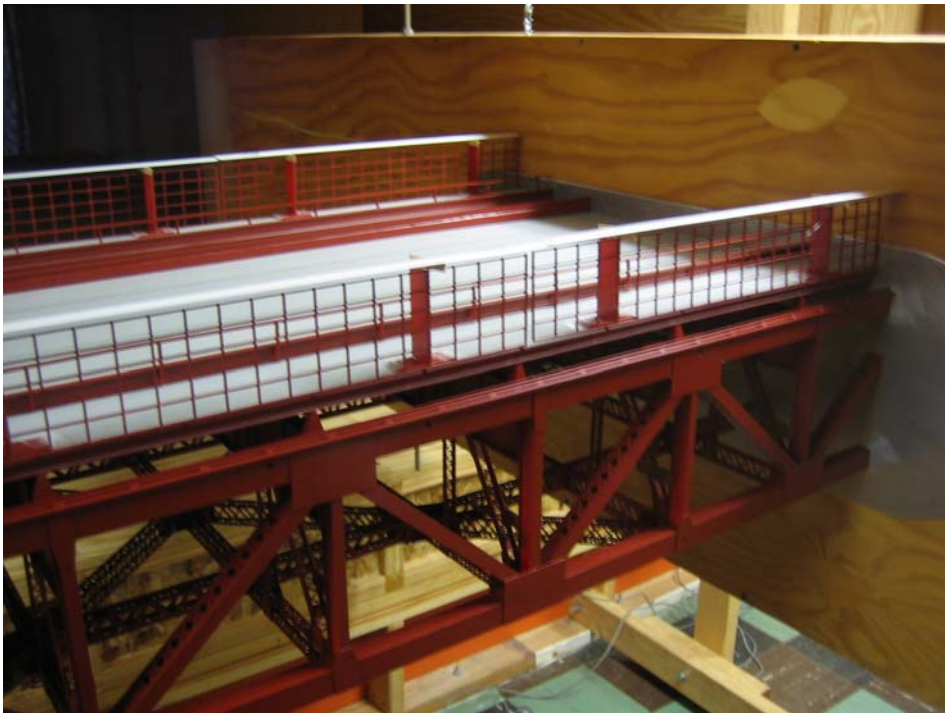
Vertical 12' barrier with wind fairings (Test number W1 Alt.)



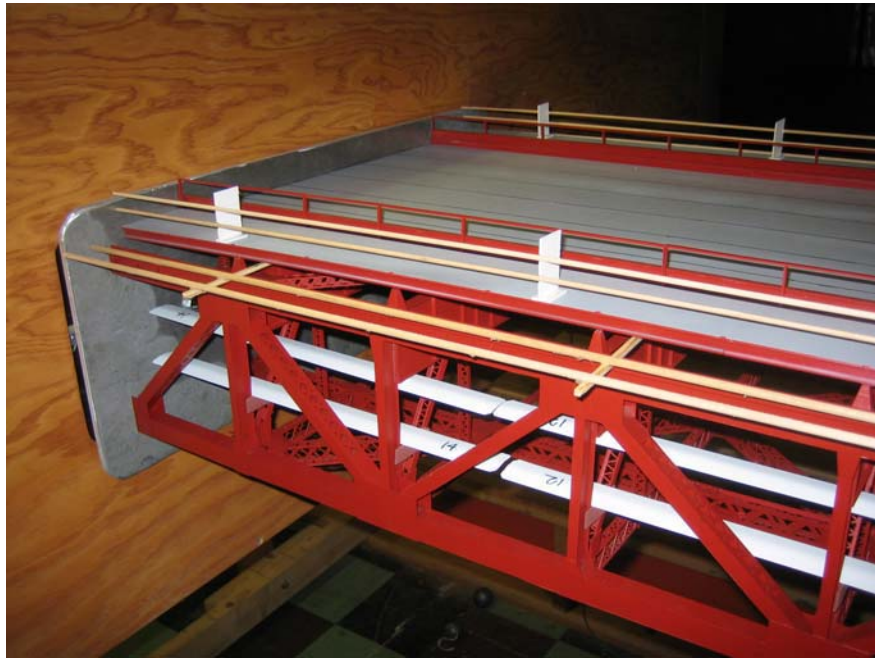
Vertical 12' barrier with above deck winglets (Test number W2)



Adding to the existing railing and with above deck winglets (Test number W3)



Vertical 10' barrier with above deck winglets (Test number W5)



Horizontally projecting 10' barrier with a modified pedestrian railing and with below deck winglets/catwalks (Test number W6)

APPENDIX 6 BRIDGE PROPERTIES

Properties of the bridge structure needed for the time domain numerical simulations are nodal coordinates, deck mass per unit length, deck mass moment of inertia about a longitudinal axis (at the center of mass), and the dynamic response characteristics (mode shapes and frequencies). The inertial properties were taken from Ref 5. The dynamic response characteristics were provided by DMJM Harris Inc. and a description of the ADINA modeling is provided below.

In a previous study on the Golden Gate Bridge, damping ratios were deduced from observed bridge motions (Ref 5). A suitable damping ratio of 0.006 was deduced. This is consistent with values of 0.004 for new steel bridges with welded and/or high strength bolted connections, and 0.005 for composite concrete and steel construction (Ref 6). Older, riveted steel truss bridges would be expected to have a higher damping value. The linear viscous damping ratio of 0.006 was therefore considered to be reasonable, and was used for all modes of vibration.

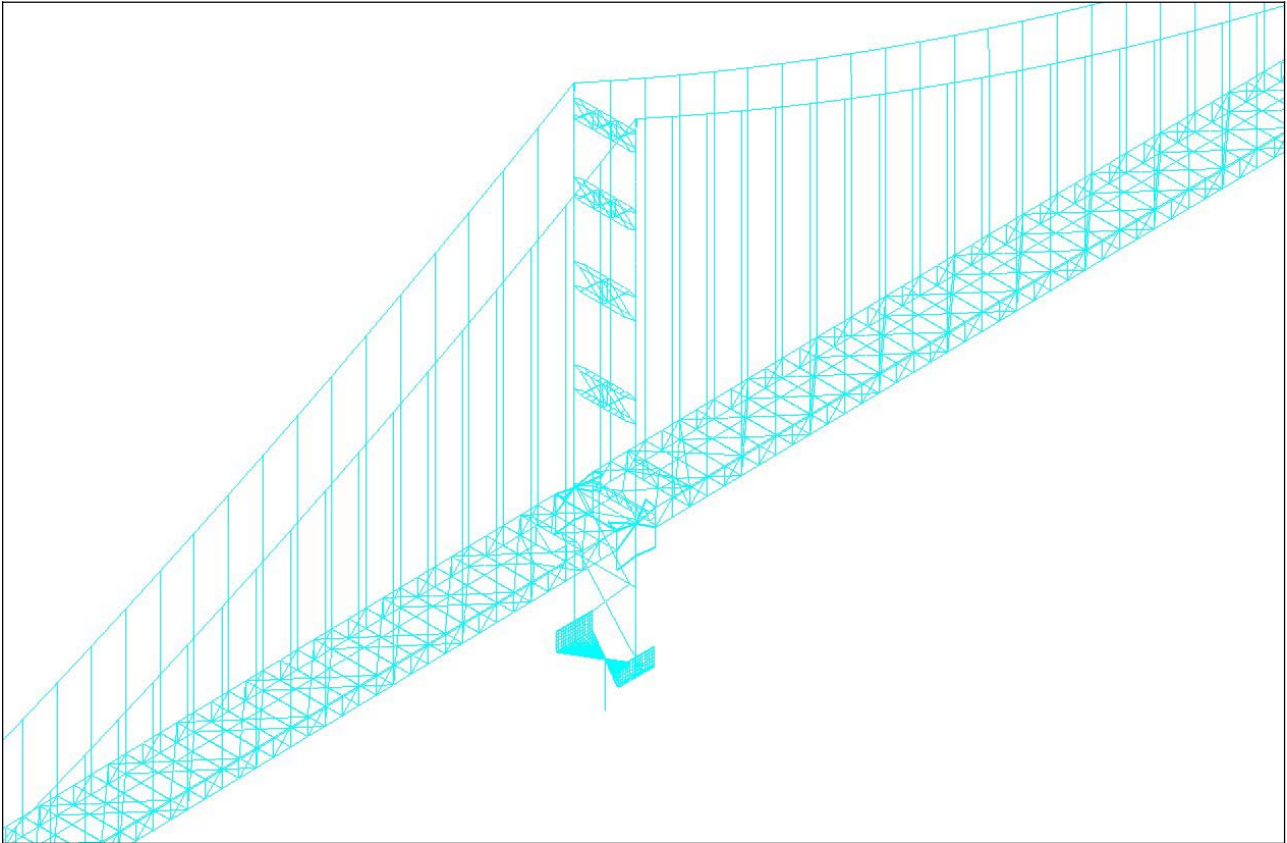
For the numerical simulations, wind speed time histories were generated at 30 locations along the span (approximately 60.96 m (200 feet) apart). Those nodal locations are defined in Table 6.1. The bridge properties used in this analysis are defined in Tables 6.2 through 6.13. The nodal locations are shown schematically in Figure 6.1. Positive coordinate directions (not standard) are shown in Figure 6.2.

ADINA Modeling

The ADINA model used for the wind stability assessment of the bridge was prepared and converted by International Civil Engineering Consultants, Inc. (ICEC) of Berkeley, California, for the Golden Gate Bridge, Highway and Transportation District (GGBHTD) of San Francisco, California, under a contract agreement by and between GGBHTD and ICEC.

The model includes the suspension bridge, the suspended main and side spans of the bridge from the North to the South anchor block. This model was developed for the modal conversion of the ABAQUS computer model for the suspended structure of the Golden Gate Bridge. It represents the structural configuration of the suspended main and side spans including with the proposed seismic retrofit of the structure.

The modeling of the suspended structure is shown in the following Figure; all major members were explicitly modeled with using linear elastic beam elements for the suspended stiffening trusses (the chords, verticals, diagonals) and the main tower (shafts, struts, verticals and diagonal braces), elastic truss elements for main cables and rocker-links, nonlinear truss elements for the suspenders, tie-downs and wind braces, nonlinear truss and member elements for the plinths (the bottom sections of the main towers), super-element (consisting of an equivalent lumped-mass matrix) for pylon, etc. Nonlinear dampers were also considered in the ADINA model.



Computation of Frequencies and Mode Shapes

The modal analysis for determining the modal frequencies with the associated mode shapes was performed using the Version of 7.4 of the ADINA computer program.

The first-twenty modal frequencies as obtained from the ADINA modal analysis are summarized in the following table.

GGB Suicide Barrier Study Frequencies per the Converted ADINA Computer Model

MODE NUMBER	FREQUENCY (Hz)	MODE SHAPE
1	0.048749	transverse, symmetric mode
2	0.086225	vertical, asymmetric mode
3	0.111783	transverse, asymmetric mode
4	0.128540	vertical, symmetric mode
5	0.133075	vertical, asymmetric mode
6	0.163712	vertical, symmetric mode
7	0.183531	torsional, asymmetric mode
8	0.195726	torsional-transverse, symmetric mode
9	0.198024	vertical, asymmetric mode
10	0.203344	cable transverse, symmetric mode
11	0.204704	torsional, symmetric mode
12	0.208492	cable transverse, asymmetric mode
13	0.211595	vertical, asymmetric mode
14	0.216478	cable transverse, asymmetric mode
15	0.224156	cable transverse, asymmetric mode
16	0.258650	vertical, symmetric mode
17	0.264104	transverse, asymmetric mode
18	0.265155	transverse, asymmetric mode
19	0.282724	vertical, symmetric mode
20	0.286409	torsional, symmetric mode

TABLE 6.1

WWL NODE	DMJM NODE
1	100580
2	101380
3	102180
4	102980
5	103780
6	105330
7	106130
8	106930
9	107730
10	108530
11	109330
12	110130
13	110930
14	111730
15	112530
16	212530
17	211730
18	210930
19	210130
20	209330
21	208530
22	207730
23	206930
24	206130
25	205330
26	203780
27	202980
28	202180
29	201380
30	200580

TABLE 6.2

B(M)= 27.432
NUMBER OF MODES= 10
NUMBER OF NODES= 30

NODE	DL(M)	M(KG/M)	MMI(KG*M^2/M)
1	60.96	29123	4.168E+06
2	60.96	29123	4.168E+06
3	60.96	29123	4.168E+06
4	60.96	29123	4.168E+06
5	60.96	29123	4.168E+06
6	60.96	29123	4.168E+06
7	60.96	29123	4.168E+06
8	60.96	29123	4.168E+06
9	60.96	29123	4.168E+06
10	60.96	29123	4.168E+06
11	60.96	29123	4.168E+06
12	60.96	29123	4.168E+06
13	60.96	29123	4.168E+06
14	60.96	29123	4.168E+06
15	60.96	29123	4.168E+06
16	60.96	29123	4.168E+06
17	60.96	29123	4.168E+06
18	60.96	29123	4.168E+06
19	60.96	29123	4.168E+06
20	60.96	29123	4.168E+06
21	60.96	29123	4.168E+06
22	60.96	29123	4.168E+06
23	60.96	29123	4.168E+06
24	60.96	29123	4.168E+06
25	60.96	29123	4.168E+06
26	60.96	29123	4.168E+06
27	60.96	29123	4.168E+06
28	60.96	29123	4.168E+06
29	60.96	29123	4.168E+06
30	60.96	29123	4.168E+06

TABLE 6.3

WWL DMJM					
MODE	MODE	WR(RPS)	DR	MT	MRAT
1	1	0.306	0.006	1.000	0.849
2	2	0.542	0.006	2.000	0.501
3	3	0.702	0.006	1.000	1.000
4	4	0.808	0.006	2.000	0.795
5	5	0.836	0.006	2.000	0.271
6	6	1.029	0.006	2.000	0.773
7	7	1.153	0.006	3.000	0.730
8	8	1.230	0.006	1.000	0.813
9	9	1.244	0.006	2.000	0.728
10	10	1.278	0.006	1.000	0.930

MT=1 FOR SWAY, 2 FOR VERTICAL, 3 FOR TORSION
MRAT IS THE RATIO OF GENERALIZED MASS ASSOCIATED WITH DECK MOTION
TO THE TOTAL GENERALIZED MASS

TABLE 6.4

WWL MODE 1
DMJM MODE 1

NODE	RX	RY	RZ
1	-0.0004	0.0000	-0.0000
2	-0.0009	0.0000	-0.0000
3	-0.0013	0.0000	-0.0000
4	-0.0015	0.0000	-0.0000
5	-0.0016	0.0000	-0.0000
6	-0.1461	0.0000	0.0000
7	-0.3033	0.0000	-0.0000
8	-0.4506	-0.0000	-0.0001
9	-0.5844	0.0000	-0.0001
10	-0.7023	0.0000	-0.0002
11	-0.8022	0.0000	-0.0002
12	-0.8827	0.0000	-0.0002
13	-0.9424	-0.0000	-0.0001
14	-0.9813	-0.0000	-0.0001
15	-1.0000	-0.0000	-0.0000
16	-1.0000	0.0000	-0.0000
17	-0.9814	0.0000	-0.0001
18	-0.9426	0.0000	-0.0002
19	-0.8830	-0.0000	-0.0002
20	-0.8025	-0.0000	-0.0002
21	-0.7025	-0.0000	-0.0002
22	-0.5843	-0.0000	-0.0001
23	-0.4503	-0.0000	-0.0001
24	-0.3031	-0.0000	-0.0000
25	-0.1459	-0.0000	0.0000
26	-0.0015	-0.0000	-0.0000
27	-0.0014	-0.0000	-0.0000
28	-0.0012	-0.0000	-0.0000
29	-0.0008	-0.0000	-0.0000
30	-0.0003	-0.0000	-0.0000

TABLE 6.5

WWL MODE 2
DMJM MODE 2

NODE	RX	RY	RZ
1	0.0001	0.0254	0.0000
2	0.0001	0.0535	-0.0000
3	0.0000	0.0642	-0.0000
4	0.0000	0.0573	-0.0000
5	0.0000	0.0334	-0.0000
6	-0.0000	0.2809	0.0000
7	-0.0001	0.5575	-0.0000
8	-0.0001	0.7770	0.0000
9	-0.0000	0.9262	0.0000
10	-0.0001	0.9951	0.0000
11	-0.0000	0.9772	0.0000
12	-0.0001	0.8732	0.0000
13	-0.0000	0.6896	0.0000
14	-0.0000	0.4406	0.0000
15	-0.0000	0.1487	0.0000
16	0.0000	-0.1579	0.0000
17	0.0001	-0.4495	0.0000
18	0.0001	-0.6978	-0.0000
19	0.0002	-0.8806	-0.0000
20	0.0003	-0.9834	-0.0000
21	0.0003	-1.0000	-0.0000
22	0.0002	-0.9299	0.0000
23	0.0001	-0.7794	-0.0000
24	0.0001	-0.5588	-0.0000
25	0.0000	-0.2813	-0.0000
26	-0.0000	-0.0329	-0.0000
27	-0.0000	-0.0564	-0.0000
28	-0.0000	-0.0633	0.0000
29	-0.0000	-0.0526	-0.0000
30	-0.0000	-0.0250	-0.0000

TABLE 6.6

WWL MODE 3
DMJM MODE 3

NODE	RX	RY	RZ
1	-0.0011	0.0000	0.0001
2	-0.0023	0.0000	0.0001
3	-0.0031	0.0000	0.0001
4	-0.0034	0.0000	0.0001
5	-0.0032	0.0000	0.0000
6	-0.2843	0.0000	0.0007
7	-0.5664	0.0001	0.0007
8	-0.7893	-0.0001	0.0007
9	-0.9352	-0.0000	0.0005
10	-0.9951	-0.0000	0.0004
11	-0.9660	-0.0001	0.0003
12	-0.8528	-0.0001	0.0001
13	-0.6658	-0.0001	0.0000
14	-0.4231	-0.0002	-0.0001
15	-0.1467	-0.0003	-0.0003
16	0.1418	-0.0001	-0.0004
17	0.4208	-0.0001	-0.0004
18	0.6662	0.0000	-0.0003
19	0.8557	0.0000	-0.0002
20	0.9704	0.0001	-0.0001
21	1.0000	0.0001	-0.0002
22	0.9393	0.0001	-0.0004
23	0.7921	0.0001	-0.0005
24	0.5681	0.0001	-0.0007
25	0.2849	0.0001	-0.0006
26	0.0029	0.0000	-0.0000
27	0.0030	0.0000	-0.0001
28	0.0028	0.0000	-0.0001
29	0.0021	0.0000	-0.0001
30	0.0010	0.0000	-0.0000

TABLE 6.7

WWL MODE 4
DMJM MODE 4

NODE	RX	RY	RZ
1	0.0003	0.1316	0.0000
2	0.0003	0.2810	-0.0000
3	0.0003	0.3397	-0.0000
4	0.0002	0.3019	-0.0000
5	0.0001	0.1743	0.0000
6	-0.0000	0.1171	-0.0000
7	-0.0000	0.1911	-0.0000
8	-0.0000	0.1798	-0.0000
9	0.0001	0.0826	0.0000
10	0.0001	-0.0863	-0.0000
11	0.0001	-0.3035	-0.0000
12	0.0001	-0.5373	-0.0000
13	0.0000	-0.7526	-0.0000
14	-0.0001	-0.9157	-0.0000
15	-0.0001	-1.0000	-0.0000
16	0.0004	-0.9920	0.0000
17	0.0003	-0.8922	0.0000
18	0.0001	-0.7158	0.0000
19	0.0000	-0.4906	0.0000
20	-0.0001	-0.2516	0.0000
21	-0.0003	-0.0343	0.0000
22	-0.0003	0.1297	0.0000
23	-0.0001	0.2178	0.0000
24	-0.0001	0.2171	0.0000
25	-0.0000	0.1297	0.0000
26	0.0001	0.1678	0.0000
27	0.0001	0.2905	-0.0000
28	0.0001	0.3268	-0.0000
29	0.0002	0.2703	-0.0000
30	0.0001	0.1265	0.0000

TABLE 6.8

WWL MODE 5
DMJM MODE 5

NODE	RX	RY	RZ
1	0.0003	0.1121	0.0000
2	0.0003	0.2396	-0.0000
3	0.0002	0.2899	-0.0000
4	0.0002	0.2575	-0.0000
5	0.0001	0.1484	0.0000
6	0.0000	-0.2509	-0.0000
7	0.0001	-0.5174	-0.0000
8	0.0002	-0.7477	-0.0000
9	0.0001	-0.9115	-0.0000
10	0.0001	-0.9845	-0.0000
11	0.0000	-0.9537	-0.0000
12	0.0001	-0.8220	-0.0000
13	0.0000	-0.6054	-0.0000
14	-0.0001	-0.3310	-0.0000
15	-0.0002	-0.0287	-0.0000
16	-0.0003	0.2734	0.0000
17	-0.0006	0.5499	0.0000
18	-0.0007	0.7769	0.0000
19	-0.0009	0.9327	0.0000
20	-0.0009	1.0000	0.0000
21	-0.0009	0.9733	0.0000
22	-0.0007	0.8585	0.0000
23	-0.0003	0.6747	0.0000
24	-0.0002	0.4493	0.0000
25	-0.0001	0.2117	0.0000
26	-0.0001	-0.1914	-0.0000
27	-0.0001	-0.3320	0.0000
28	-0.0002	-0.3736	0.0000
29	-0.0002	-0.3088	0.0000
30	-0.0001	-0.1443	-0.0000

TABLE 6.9

WWL MODE 6
DMJM MODE 6

NODE	RX	RY	RZ
1	0.0007	0.2673	0.0000
2	0.0008	0.5797	0.0000
3	0.0007	0.7064	-0.0000
4	0.0005	0.6265	-0.0000
5	0.0002	0.3581	0.0000
6	-0.0000	-0.3399	0.0000
7	0.0001	-0.6736	0.0000
8	0.0001	-0.9080	0.0000
9	-0.0001	-0.9962	-0.0000
10	-0.0001	-0.9206	-0.0000
11	-0.0001	-0.6961	0.0000
12	-0.0001	-0.3728	0.0000
13	-0.0000	-0.0233	0.0000
14	0.0001	0.2700	0.0000
15	0.0002	0.4362	-0.0000
16	-0.0007	0.4358	-0.0000
17	-0.0005	0.2687	-0.0000
18	-0.0001	-0.0255	-0.0000
19	0.0002	-0.3758	-0.0000
20	0.0005	-0.6997	-0.0000
21	0.0006	-0.9245	-0.0000
22	0.0006	-1.0000	-0.0000
23	0.0002	-0.9111	-0.0000
24	0.0002	-0.6757	-0.0000
25	0.0001	-0.3408	-0.0000
26	0.0001	0.3625	0.0000
27	0.0002	0.6340	0.0000
28	0.0003	0.7149	-0.0000
29	0.0003	0.5866	0.0000
30	0.0002	0.2705	0.0000

TABLE 6.10

WWL MODE 7
DMJM MODE 7

NODE	RX	RY	RZ
1	0.0027	-0.0000	-0.0003
2	0.0049	-0.0000	-0.0006
3	0.0059	-0.0000	-0.0007
4	0.0058	-0.0000	-0.0006
5	0.0045	-0.0000	-0.0004
6	-0.1171	0.0001	0.0221
7	-0.1827	0.0000	0.0412
8	-0.2264	0.0004	0.0568
9	-0.2438	0.0001	0.0677
10	-0.2375	-0.0002	0.0729
11	-0.2111	-0.0002	0.0718
12	-0.1692	-0.0002	0.0645
13	-0.1160	-0.0001	0.0517
14	-0.0571	0.0005	0.0346
15	0.0030	0.0015	0.0145
16	0.0507	0.0007	-0.0072
17	0.0865	0.0003	-0.0286
18	0.1138	0.0001	-0.0474
19	0.1335	0.0001	-0.0618
20	0.1467	0.0001	-0.0704
21	0.1549	0.0001	-0.0725
22	0.1570	0.0001	-0.0678
23	0.1486	0.0002	-0.0572
24	0.1243	-0.0000	-0.0417
25	0.0875	-0.0000	-0.0223
26	-0.0008	-0.0001	-0.0003
27	-0.0008	-0.0002	-0.0004
28	-0.0006	-0.0003	-0.0005
29	-0.0002	-0.0002	-0.0004
30	0.0003	-0.0001	-0.0002

TABLE 6.11

WWL MODE 8
DMJM MODE 8

NODE	RX	RY	RZ
1	0.0608	-0.0000	-0.0103
2	0.0982	0.0001	-0.0194
3	0.1124	0.0004	-0.0228
4	0.1052	0.0005	-0.0205
5	0.0756	0.0006	-0.0128
6	-0.3503	0.0001	-0.0012
7	-0.6804	0.0002	-0.0002
8	-0.8943	0.0001	0.0049
9	-0.9601	-0.0004	0.0140
10	-0.8780	-0.0009	0.0260
11	-0.6736	-0.0012	0.0399
12	-0.3958	-0.0012	0.0540
13	-0.1041	-0.0008	0.0669
14	0.1376	-0.0006	0.0769
15	0.2742	-0.0003	0.0832
16	0.2786	0.0001	0.0850
17	0.1453	0.0005	0.0819
18	-0.1002	0.0007	0.0741
19	-0.4021	0.0008	0.0625
20	-0.6935	0.0006	0.0487
21	-0.9111	0.0003	0.0344
22	-1.0000	-0.0002	0.0214
23	-0.9320	-0.0005	0.0111
24	-0.7094	-0.0005	0.0043
25	-0.3672	-0.0003	0.0012
26	0.0770	0.0002	-0.0131
27	0.1074	-0.0002	-0.0210
28	0.1149	-0.0004	-0.0233
29	0.1005	-0.0005	-0.0198
30	0.0622	-0.0003	-0.0105

TABLE 6.12

WWL MODE 9
DMJM MODE 9

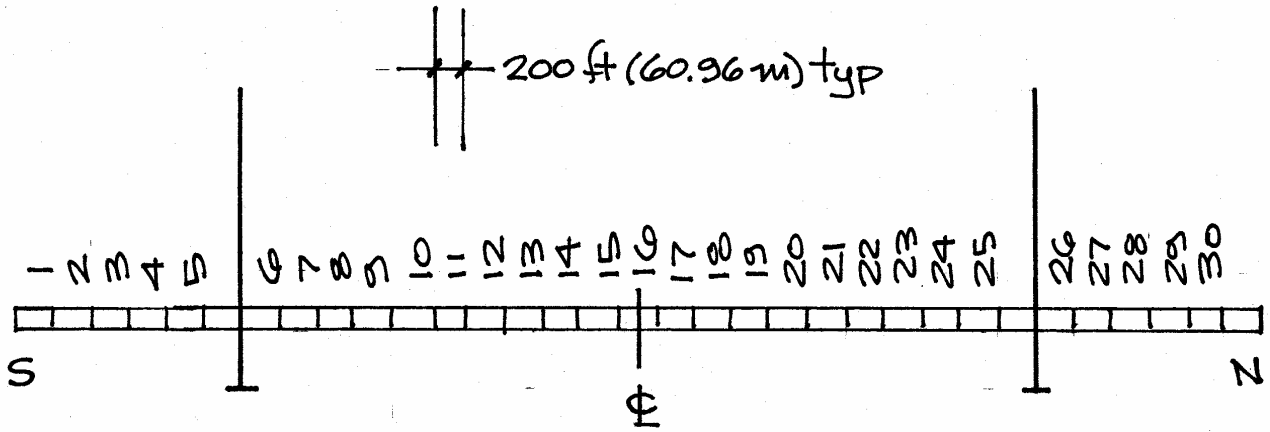
NODE	RX	RY	RZ
1	0.0011	0.3666	0.0000
2	0.0014	0.8117	-0.0000
3	0.0013	1.0000	-0.0000
4	0.0010	0.8854	-0.0000
5	0.0005	0.5005	0.0000
6	0.0001	0.0469	-0.0000
7	0.0003	0.0835	-0.0000
8	0.0003	0.0915	-0.0000
9	0.0004	0.0704	-0.0000
10	0.0004	0.0289	-0.0000
11	0.0003	-0.0190	-0.0000
12	0.0001	-0.0572	-0.0000
13	-0.0000	-0.0724	-0.0000
14	-0.0001	-0.0591	-0.0000
15	-0.0002	-0.0227	-0.0000
16	-0.0002	0.0226	-0.0000
17	-0.0002	0.0590	0.0000
18	-0.0000	0.0721	0.0000
19	0.0001	0.0568	0.0000
20	0.0003	0.0185	0.0000
21	0.0004	-0.0295	0.0000
22	0.0005	-0.0710	0.0000
23	0.0004	-0.0919	0.0000
24	0.0003	-0.0838	0.0000
25	0.0001	-0.0470	0.0000
26	-0.0002	-0.4968	-0.0000
27	-0.0004	-0.8790	0.0000
28	-0.0005	-0.9928	0.0000
29	-0.0005	-0.8061	0.0000
30	-0.0003	-0.3642	-0.0000

TABLE 6.13

WWL MODE 10
DMJM MODE 10

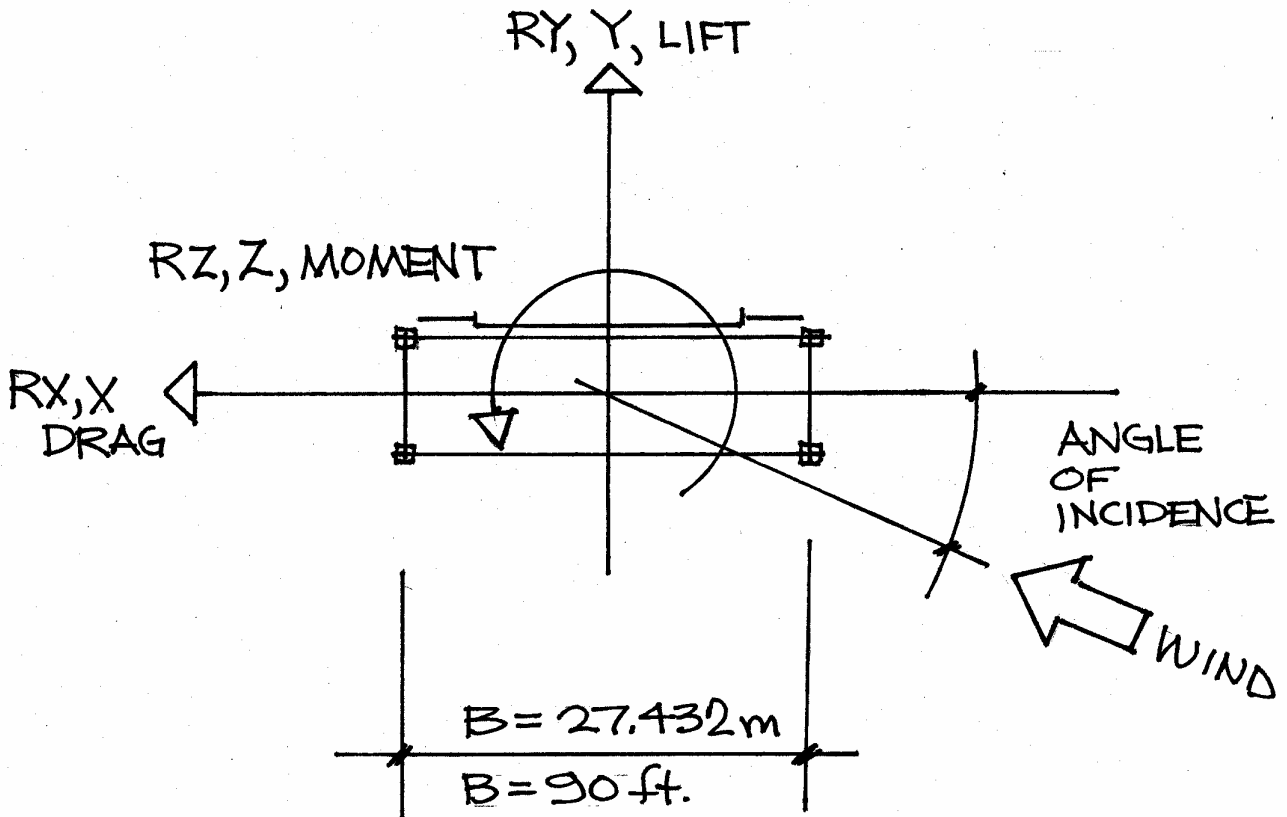
NODE	RX	RY	RZ
1	0.0585	-0.0004	-0.0095
2	0.0960	-0.0008	-0.0179
3	0.1106	-0.0008	-0.0210
4	0.1035	-0.0006	-0.0189
5	0.0740	-0.0001	-0.0118
6	0.4239	0.0008	-0.0019
7	0.7931	0.0012	0.0010
8	0.9919	0.0016	0.0079
9	0.9917	0.0009	0.0178
10	0.8015	-0.0001	0.0297
11	0.4594	-0.0009	0.0421
12	0.0320	-0.0015	0.0537
13	-0.3981	-0.0017	0.0635
14	-0.7451	-0.0012	0.0706
15	-0.9370	-0.0003	0.0741
16	-0.9374	0.0007	0.0738
17	-0.7448	0.0016	0.0696
18	-0.3954	0.0020	0.0621
19	0.0383	0.0016	0.0521
20	0.4688	0.0008	0.0403
21	0.8116	-0.0003	0.0279
22	1.0000	-0.0013	0.0160
23	0.9976	-0.0019	0.0062
24	0.7972	-0.0016	-0.0003
25	0.4264	-0.0009	-0.0026
26	0.0738	0.0007	-0.0121
27	0.1037	0.0008	-0.0193
28	0.1110	0.0007	-0.0215
29	0.0967	0.0004	-0.0183
30	0.0591	0.0001	-0.0097

Figure 6.1



WEST WIND LABORATORY NODE NUMBERS

Figure 6.2



POSITIVE COORDINATE DIRECTIONS

APPENDIX 7 REFERENCES

1. Simiu, E., and Scanlan, R. H. Wind Effects on Structures, Third Edition, John Wiley & Sons, New York, 1996.
2. Raggett, J. D., West Wind Laboratory, Inc., "Section Model Wind Tunnel Studies Golden Gate Bridge Seismic and Wind Retrofit, San Francisco, California", Job No. W920421, June 1995
3. Yinghong Cao, Haifan Xiang, and Ying Zhou, "Simulation of Stochastic Wind Velocity Field on Long-Span Bridges", Journal of Engineering Mechanics, Vol. 126, No. 1, ASCE, January, 2000
- 4.. Xinzhong Chen, Masaru Matsumoto, and Ahsan Kareem, "Time Domain Flutter and Buffeting Response Analysis of Bridges", Journal of Engineering Mechanics, Vol. 126, No. 1, ASCE, January, 2000
5. Xie, J., Dunn, G., Irwin, P. A., Rowan Williams Davies & Irwin Inc., "Wind Tunnel Studies for the Golden Gate Bridge, San Francisco, California", Report 93-144F-5, April 20, 1994
6. British Highways Agency, Design Manual for Roads and Bridges, BD 37/01, Loads for Highway Bridges.
7. Raggett, J. D., "Stabilizing Winglet Pair for Slender Bridge Decks", Proceedings of the 6th Annual ASCE Structural Division Structures Congress, August 17-20, 1987

